Electronic Supplementary Material (ESI) for Physical Chemistry Chemical Physics.

On the transferability of classical pairwise additive atomistic force field to the description of unary and multi-component systems: Applications to the solidification of Al-based alloys

Juan-Ricardo Castillo-Sánchez, Antoine Rincent, Aïmen E. Gheribi, and Jean-Philippe Harvey*

**Corresponding Author:* jean-philippe.harvey@polymtl.ca

Centre for Research in Computational Thermochemistry (CRCT), Department of Chemical Engineering, Polytechnique Montréal, C.P. 6079, Succursale "Downtown", Montréal, Québec H3C 3A7, Canada.

1. TITANIUM-ZIRCONIUM PHASE DIAGRAM

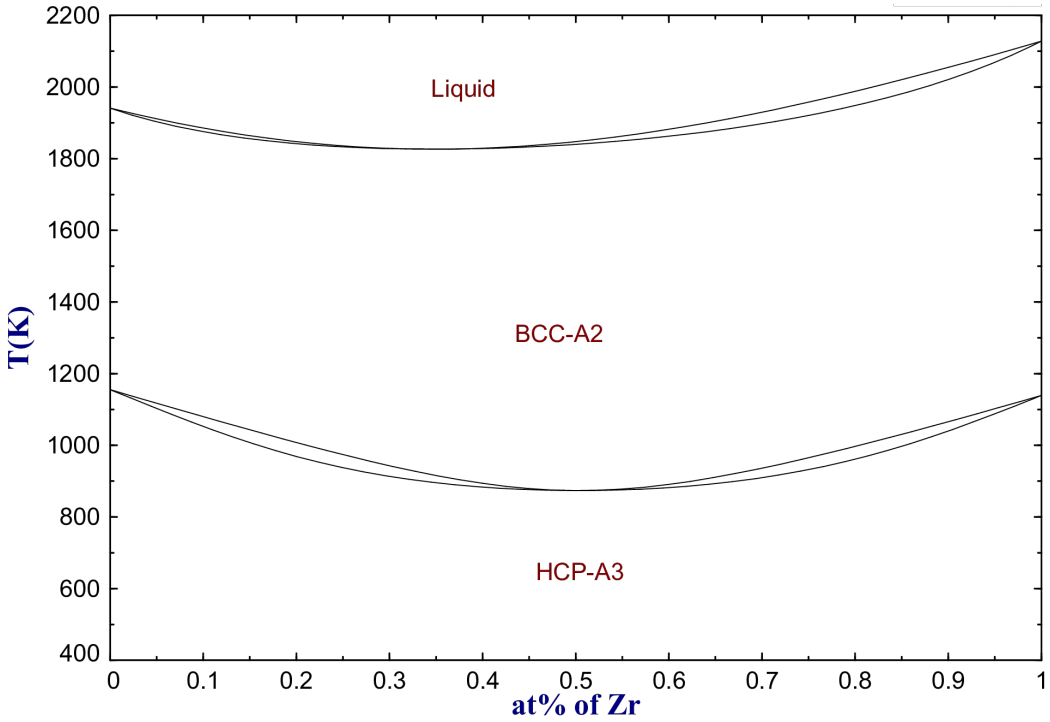

Fig. S1. Ti-Zr phase diagram computed with Factsage [1].

2. INITIAL CONFIGURATION FOR MD SIMULATIONS OF ALUMINIUM-CHROMIUM ALLOYS

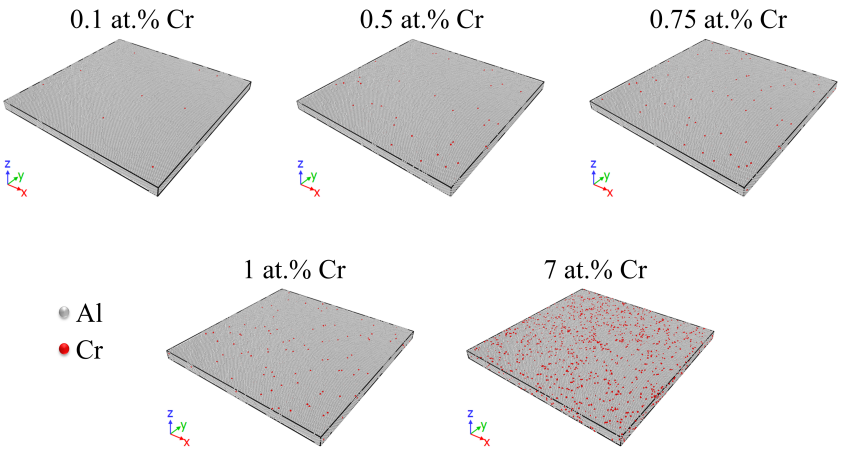

Fig. S2. Representation of the initial configurations for the simulations of Al-Cr alloys (Al atoms are presented in grey, Cr atoms are in red). Cr atoms were randomly distributed across an FCC simulation box followed by a volume minimization.

3. ALUMINIUM-CHROMIUM PHASE DIAGRAM

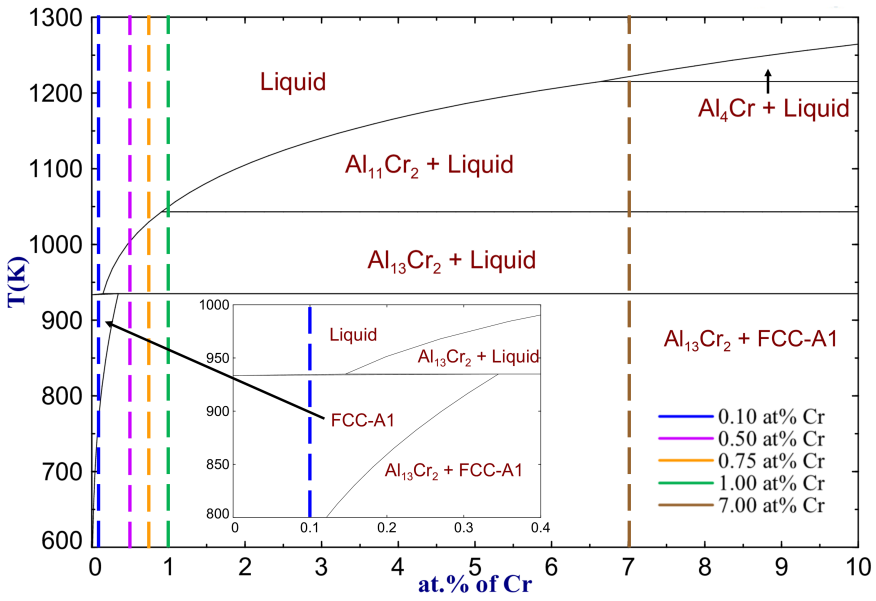

Fig. S3. Computed Al-Cr phase diagram using the FTlite database [1]. The different compositions studied in this work are indicated with dashed lines.

4. ENERGETICS OF PARTIALLY ORDERED $D0_{22}$ AND $D0_{23}$ SOLID SOLUTIONS

Our last series of MD simulations is related to the energetic description of partially ordered Al_3(Zr,Ti)-$D0_{23}$ and Al_3(Ti,Zr)-$D0_{22}$ solid solutions, which are of prime importance in aluminum alloys [2–5]. The modeling was first carried out with first-principle calculations. Results were after compared to MD predictions using the Al-Zr-Ti interatomic potential developed in this work.

A. Solution modelling

The Vienna ab initio Simulation Package (VASP) [6–9] has been used to perform the plane wave density functional theory (DFT) simulations to determine the enthalpy of formation and the lattice constants of both Al_3(Ti,Zr) in both $D0_{22}$ and $D0_{23}$ structures. Pseudopotentials constructed by the projector-augmented wave (PAW) method originally proposed by Blöchl [10, 11] were employed for Al, Ti and Zr. The generalized gradient approximation (GGA) of Perdew, Burke and Ernzerhof (PBE) [12, 13] has been considered to describe the exchange-correlation functionals. Convergence in the energy and cell volume was achieved by using a cut-off energy of 520 eV. The Monkhorst-Pack scheme was used to sample the Brillouin zone with a 3 × 3 × 1 k-point mesh for both $D0_{22}$ and $D0_{23}$ structures. Zone with a Gaussian smearing parameter σ of 0.02 eV ensure that the accuracy in the energy of the system is more than 0.01 meV. The self-consistent field (SCF) convergence criterion was 1x10^{-5} eV for electronic iteration and 0.02 eV/Å for each ionic loop that was updated by the conjugate gradient approach. The total energy has been calculated in the NPT statistical ensemble, i.e the equilibrium lattice, the atomic positions, cell volume and cell shape, all were free to be relaxed. A total of 128 and 256 atoms have been considered for $D0_{22}$ and $D0_{23}$ structures respectively. Several configurations in which Ti and Zr were randomly substituted have been generated. Volume optimization for MD simulations was performed using the equilibrated supercells from DFT as initial configurations. The corresponding 0 K molar enthalpy of mixing (Δh_f^{soln}) have been determined as:

$$\Delta h_f^{soln} = h_{Al_3Y_{1-x}Z_x} - (1-x)h_{Al_3Y}^{Ref-0K} - xh_{Al_3Z}^{CSS-0K} \quad \text{(S1)}$$

In this equation, $h_{Al_3Y_{1-x}Z_x}$ is the molar enthalpy of the minimized pseudo-binary solid solution at 0 K, computed by volume minimization (with Y=Zr and Z=Ti for the $D0_{23}$ phase and vice-versa for the $D0_{22}$ phase). The fraction of sub-lattice substitution of Z sites by Y atoms in the tetragonal phases is defined in this equation by x. The $h_{Al_3Y}^{Ref-0K}$ expression represents the molar enthalpy of the binary stable reference structure at 0K while $h_{Al_3Z}^{CSS-0K}$ refers to the molar enthalpy of the reference structure with complete sub-lattice substitution of Y atoms by Z atoms.

B. Results

Intermetallics are commonly found as partially ordered multicomponent solid solutions in typical solidified aluminum alloy microstructures. For example, Al_3Zr-based intermetallics have been identified as nucleant particles of the FCC-phase of aluminum alloys. More precisely, they have been found at the core of α-grains within the 6082 Aluminum Alloy [4]. Al_3Zr intermetallics reported in that study contained important amounts of Ti which substituted Zr in specific sub-lattices. This partially ordered structure is a result of atomic substitutions of specific elements of their perfectly ordered structure by either alloying elements or impurities. This substitution can be energetically described by thermodynamic models such as the compound energy formalism [14]. In the context of a solidification process, such partial substitutions in a given primary phase can lead to stabilization entropy effects [15] that may impact the nucleation process. This section explores the structural and energetic behavior of Al_3Zr-$D0_{23}$ and Al_3Ti-$D0_{22}$ intermetallics that experience atomic substitution within their crystal structure. These two intermetallic phases were specifically chosen as they are of critical importance when studying the solidification process and resulting mechanical behaviour of various aluminum alloys. More specifically, elastic properties and lattice parameters of both Al_3Zr-$D0_{22}$ and Al_3Ti-$D0_{23}$ tetragonal phases evaluated at 0K are presented in Table S1. The energetic description of both perfect crystal structures obtained from the MEAM force field models used in this work are in excellent agreement with the DFT calculations reported in the literature. Elastic constants and lattice parameters for the cubic the Zr_2TiAl (Fm3m) compound were also computed (Table S1). The interatomic potentials used in our work provide an adequate description of this isotropic ternary compound when compared to DFT results found in the literature [16]. Based on these results, it is assumed that the pseudo-binary

solid solutions modeled with these MEAM force field models should provide precise energetic results.

Table S1. Lattice parameters and elastic constant of Al_3Zr-$D0_{23}$, Al_3Ti-$D0_{22}$ and Zr_2TiAl compounds by MD simulations compared to DFT calculations.

	Al_3Zr-$D0_{23}$		Al_3Ti-$D0_{22}$		Zr_2TiAl ($Fm\bar{3}m$)	
	MEAM (this work)	DFT [17, 18]	MEAM (this work)	DFT [17, 18]	MEAM (this work)	DFT [16]
Lattice parameter "a" (Å)	4.05	4.02	3.89	3.84	6.72	6.81
Lattice parameter "c" (Å)	17.46	17.24	8.71	8.60	...	...
B (GPa)	96.20	103	124	92	108.74	101.249
C_{11} (GPa)	145.01	209	145.81	196	145.81	119.414
C_{12} (GPa)	82.76	64	143.28	87	90.20	92.167
C_{13} (GPa)	71.16	45	80.67	45	90.20	...
C_{44} (GPa)	39.65	81	52.58	93	84.77	64.186
Poisson ratio	0.35	0.18	0.38	0.18	0.38	0.31

Simulations supercells of 128 atoms were used for the exploration of the energetic behaviour of the $Al_3(Zr_x,Ti_{1-x})$-$D0_{23}$ solid solution while 256 atoms were used for the $Al_3(Ti_x,Zr_{1-x})$-$D0_{22}$ structure. The *a* and *c* lattice parameters, as well as the enthalpy of formation of both tetragonal solid solutions, were computed with EMD and DFT calculations via 0K volume minimization (Figure S4 and Figure S5). It is to be noted that the initial atomic configurations accounting for Ti and Zr substitution were exactly the same for both MD and DFT simulations. Lattice constants were compared to the one of pure Al FCC from DFT calculations at 0K [17] in all our figures. Figure S4a shows the evolution of the *a* parameter in the $D0_{23}$-phase as Zr is substituted by Ti. This cell parameter decreases as Zr atoms are substituted. This is consistent with the different atomic radii of Zr and Ti. The same behavior is observed for the *c* lattice parameter (Figure S4b). Our results show that the *a* parameter of the perfectly ordered $D0_{23}$ structure is virtually the same as the lattice parameter of the pure FCC aluminum matrix. This figure also shows that the *c* lattice parameter is more than 4 times bigger than the lattice parameter of pure FCC aluminum. This high lattice mismatch between the FCC and $D0_{23}$ in the z-direction is slightly reduced as Zr sites are substituted by Ti. The opposite trend is observed for the *a* parameter of this $D0_{23}$ structure. From an energetic perspective, the substitution of Zr by Ti is not energetically favored according to our DFT simulations (Figure S4c) while the classical MD simulations predicted an almost null enthalpy effect upon these atomic substitutions. The small energetic enthalpy barrier predicted by DFT can easily be overcome when increasing temperature due to configurational entropy effects. Therefore it is reasonable to assume that Zr substitutions by Ti (which is experimentally observed) stabilize this structure via configurational entropy effects [15]. At lower temperatures, there is a driving force for this structure to order.

Equivalent conclusions were obtained for the modeling of the pseudo-binary $Al_3(Ti,Zr)$-$D0_{22}$ solid solution (Figure S5). For this system, it is found that the *c* parameter is more than two times the FCC aluminum lattice parameter (Figure S5b). Precipitation of the Al_3Ti-$D0_{22}$ tetragonal phase particularly is energetically favored by the electronic hybridation between Al *p* and Ti *d* electrons. This promotes the formation of this partially symmetrical $D0_{22}$ structure over the cubic Al_3Ti-$L1_2$ phase [19]. As such, the parameterized MEAM potential is not able to account for this specific electronic phenomenon due to the simplifications regarding the description of the electronic structure representation. In this case, DFT simulations should provide a more realistic description of the Al_3Ti-$D0_{22}$ at 0K. Surprisingly, precise results are obtained with our MD simulations when compared to DFT. Overall, the determination of other inter-planar distances should be assessed in future work to better understand the effect of these lattice mismatches on the energetic stability of this phase. Dilatation effects upon heating of the FCC and $D0_{23}$ phases should also be considered as they will also influence these results.

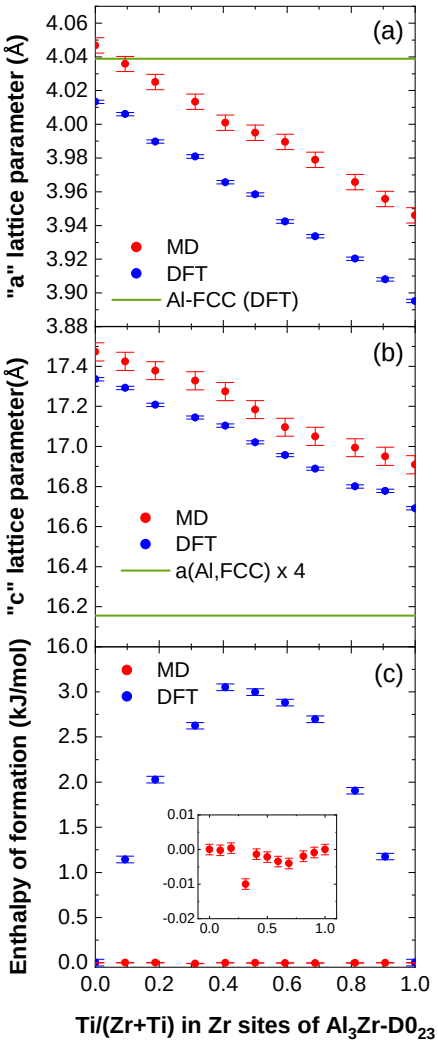

Fig. S4. Pseudo-binary $Al_3(Zr,Ti)$-$D0_{23}$ solid solution

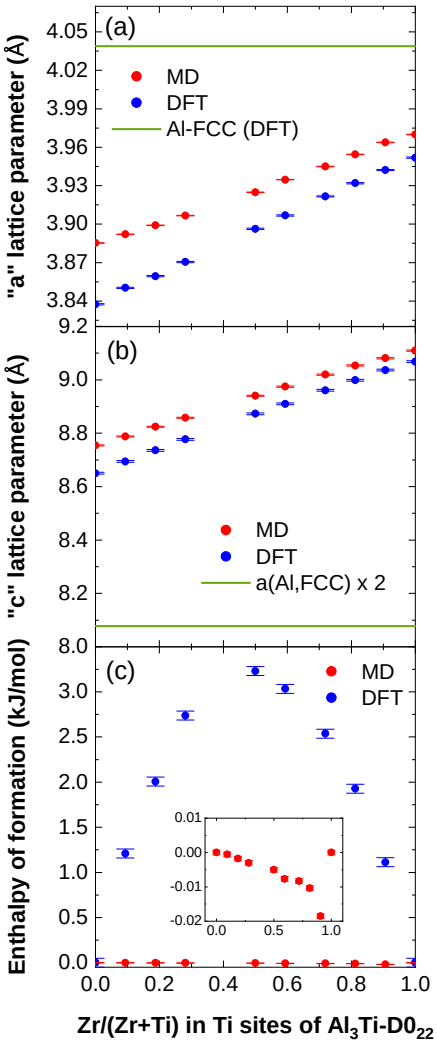

Fig. S5. Pseudo-binary $Al_3(Ti,Zr)$-$D0_{22}$ solid solution.

REFERENCES

1. C. W. Bale, P. Chartrand, S. Degterov, G. Eriksson, K. Hack, R. B. Mahfoud, J. Melançon, A. Pelton, and S. Petersen, "Factsage thermochemical software and databases," Calphad **26**, 189–228 (2002).
2. F. Crossley and L. Mondolfo, "Mechanism of grain refinement in aluminum alloys," JOM **3**, 1143–1148 (1951).
3. F. Wang, D. Qiu, Z.-L. Liu, J. A. Taylor, M. A. Easton, and M.-X. Zhang, "The grain refinement mechanism of cast aluminium by zirconium," Acta materialia **61**, 5636–5645 (2013).
4. G. Salloum-Abou-Jaoude, D. Eskin, C. Barbatti, P. Jarry, M. Jarrett, and Z. Fan, "Effect of ultrasonic processing on a direct chill cast AA6082 aluminium alloy," in *Light Metals 2017*, (Springer, 2017), pp. 997–1003.
5. Z. Chen and K. Yan, "Grain refinement of commercially pure aluminum with addition of Ti and Zr elements based on crystallography orientation," Sci. Reports **10**, 1–8 (2020).
6. G. Kresse and J. Hafner, "Ab initio molecular dynamics for liquid metals," Phys. review B **47**, 558 (1993).
7. G. Kresse and J. Hafner, "Ab initio molecular-dynamics simulation of the liquid-metal–amorphous-semiconductor transition in germanium," Phys. Rev. B **49**, 14251 (1994).
8. G. Kresse and J. Furthmüller, "Efficiency of ab-initio total energy calculations for metals and semiconductors using a plane-wave basis set," Comput. materials science **6**, 15–50 (1996).
9. G. Kresse and J. Furthmüller, "Efficient iterative schemes for ab initio total-energy calculations using a plane-wave basis set," Phys. review B **54**, 11169 (1996).
10. P. E. Blöchl, "Projector augmented-wave method," Phys. review B **50**, 17953 (1994).
11. G. Kresse and D. Joubert, "From ultrasoft pseudopotentials to the projector augmented-wave method," Phys. review b **59**, 1758 (1999).
12. J. P. Perdew, K. Burke, and M. Ernzerhof, "Generalized gradient approximation made simple," Phys. review letters **77**, 3865 (1996).
13. J. P. Perdew, K. Burke, and M. Ernzerhof, "Generalized Gradient Approximation made simple [phys. rev. lett. 77, 3865 (1996)]," Phys. Rev. Lett. **78**, 1396–1396 (1997).
14. M. Hillert, "The compound energy formalism," J. Alloy. Compd. **320**, 161–176 (2001).
15. P. Lafaye, K. Oishi, M. Bourdon, and J.-P. Harvey, "Crystal chemistry and thermodynamic modelling of the Al13(Fe,TM)4 solid solutions (TM = Co, Cr, Ni, Pt)," J. Alloy. Compd. p. 165779 (2022).
16. N.-A. Vahabzadeh, A. Boochani, S. M. Elahi, and H. Akbari, "Structural, Half-Metallic, Optical, and Thermoelectric Study on the Zr2TiX (X= Al, Ga, Ge, Si) Heuslers: by DFT," Silicon **11**, 501–511 (2019).
17. A. Jain, S. P. Ong, G. Hautier, W. Chen, W. D. Richards, S. Dacek, S. Cholia, D. Gunter, D. Skinner, G. Ceder *et al.*, "Commentary: The Materials Project: A materials genome approach to accelerating materials innovation," APL materials **1**, 011002 (2013).
18. M. De Jong, W. Chen, T. Angsten, A. Jain, R. Notestine, A. Gamst, M. Sluiter, C. Krishna Ande, S. Van Der Zwaag, J. J. Plata *et al.*, "Charting the complete elastic properties of inorganic crystalline compounds," Sci. data **2**, 1–13 (2015).
19. J.-Y. Park, I.-H. Kim, A. T. Motta, C. J. Ulmer, M. A. Kirk Jr, E. A. Ryan, and P. M. Baldo, "Irradiation-induced disordering and amorphization of Al_3Ti-based intermetallic compounds," J. Nucl. Mater. **467**, 601–606 (2015).